ELEVENTH EUROPEAN ROTORCRAFT FORUM

Paper No. 39

The Development of Advanced Technology Blades For Tiltrotor Aircraft

Harold R. Alexander
Boeing Vertol Company
Philadelphia, Pennsylvania, U.S.A.

Martin D. Maisel
Aeromechanics Laboratory
AVSCOM, Ames Research Center
Moffett Field, California, U.S.A

Demo J. Giulianetti
NASA, Ames Research Center
Moffett Field, California, U.S.A.

September 10-13, 1985
London, England.

THE CITY UNIVERSITY, LONDON, EC1V OHB, ENGLAND.

THE DEVELOPMENT OF ADVANCED TECHNOLOGY BLADES FOR TILTROTOR AIRCRAFT

Harold R. Alexander
Boeing Vertol Company
Philadelphia, PA, U.S.A.

Martin D. Maisel
AVSCOM, Ames Research Center
Moffett Field, CA, U.S.A.

Demo J. Giulianetti
NASA, Ames Research Center
Moffett Field, CA, U.S.A.

Abstract

The paper discusses the development and ground testing of blades for the XV-15 tiltrotor demonstrator aircraft. This work was performed under Contract NAS2 11250 with the NASA Ames Research Center. These blades, known as the Advanced Technology Blades (ATB), replace the rectangular steel blades which were part of the XV-15 original design. The materials used in the primary structure of the ATB are fiberglass and high strain graphite epoxy laminates. This facilitates the use of 43 degrees of non-linear twist, a nonuniform tapered planform and thin airfoils required for aerodynamic efficiency. Instrumentation life is extended by encapsulating gages and wiring in the composite structure. Tip shells and cuff fairings are removable to provide access to tip weights and retention hardware; they are also replaceable with alternate research configurations. Extensive laboratory testing has validated predicted strength characteristics. Hover testing has demonstrated performance significantly superior to that predicted by contemporary methodology. Key elements of the test rig used for rotor performance measurement were developed as an ancillary part of the present program. The performance testing included measurement of near- and far-field noise. Induced inflow velocity distributions were also determined and photographs of tip vortex condensation trails were taken. These are providing guidance for modifications to hover performance codes.

Introduction

Background

In the early 1970's, the United States National Aeronautics and Space Administration undertook the development and flight demonstration of a tiltrotor technology research aircraft. This initiative culminated in the very successful XV-15 tiltrotor research aircraft which achieved first flight in 1977. The flight test program which ensued has demonstrated in a definitive manner the engineering feasibility of the tiltrotor concept as a flight vehicle with the vertical take-off and landing capability of the helicopter and the cruise capability of the conventional fixed wing aircraft. Figure 1 shows the XV-15 in its various operating modes.

The success of the XV-15 program has fostered a growing interest in the tilt rotor concept for a number of military and commercial applications. Because of the importance of rotor performance and structural integrity to the operating parameters of tilt rotor aircraft, a research and development program was initiated at NASA Ames Research Center in 1982 to develop blades for the XV-15, exploring the most advanced technology available. These blades are customarily referred to as the XV-15 Advanced Technology Blades or ATB for short. They will replace the currently installed 14 in. (0.356m) chord rectangular steel blades. Figure 2 shows the main features of the ATB which include nonuniform taper, 43 degrees of non-linear twist and detachable tips and cuffs. The ATB has a solidity of 0.103 compared with 0.089 for the steel blades. The diameter of both rotors is 25 ft. (7.62m)

The XV-15 airframe and current rotor system is based on 1960's materials technology. In particular the rotor blades are of stainless steel and aluminum honeycomb core construction. These blades were developed for an aircraft of 9500 pounds (4309 kilograms) design gross weight. A substantial amount of blade qualification testing had been accomplished when the aircraft weight was increased to 13,000 pounds (5897 kilograms). The blades were considered adequate for the higher weight and the design was retained in the interest of program cost and schedule.

As the flight test program of the XV-15 progressed it became apparent that it would extend beyond the projected life of the original blade sets, and a replacement blade development program was initiated. These new blades would take account not only of the nominal design gross weight but also the desire for even higher operating weights and improved maneuver load factor in the helicopter and transition modes of operation.

In the years since the fabrication of the XV-15 steel rotor blades, the use of composite materials has become widespread in helicopter blade manufacture. It was determined that the new replacement blades for the XV-15 would exploit fully the improvements made available by composite technology. This would include performance advantages of unconventional planforms and the strength and fatigue advantages of designing in composite material as compared with metal. Because of the differences in twist and planform between blades designed solely for the helicopter mode of operation and those designed for vertical takeoff and subsequent cruise in a propeller mode, the application of composites in tilt rotor blade design challenged and extended the state of the art in a number of ways which will be discussed in the body of the paper.

Thus the blade program which was finally formulated not only addressed the immediate needs of the XV-15 tilt rotor demonstrator aircraft but also included a distinct research and development dimension in the areas of aerodynamics, structures, dynamics and manufacturing technology.

Contractual Objectives

These aspirations for the ATB program were summarized in a set of formal contractual objectives as follows:

- Maximize the XV-15 productivity coefficient defined as:

$$P = \frac{\text{Payload X Cruise Speed}}{\text{Weight Empty}}$$

  consistent with existing engines, transmission and structural design limits, and subject also to the requirement that the high speed airplane mode performance not be degraded.

- Improve blade fatigue strength and thereby extend service life and expand the transition flight envelope in areas where it is currently limited by blade strength.

- Demonstrate feasibility of manufacturing processes for highly twisted composite tilt rotor blades of unconventional design.

- Demonstrate structural properties, rotor performance and blade loads by ground and flight test evaluation.

The paper discusses the approaches to, and the measure of success to date, in accomplishing these objectives.

Performance

The use of molded composite material relaxes many of the constraints on design which routinely apply with metal structures, and aerodynamics design can more nearly approach the ideal without incurring unacceptable cost. Thus the ATB uses non-linear twist, a nonuniform tapered planform and thin section airfoils, selected to provide the hover and cruise performance objectives. The blade planform selected is shown in Figure 3 along with the distribution of airfoil sections. Figures 4, 5, and 6 show the twist, thickness ratio and chord distributions for the XV-15 steel blades and for the ATB. A detailed technical background to the selection of the ATB aerodynamic design parameters is given in Reference 1.

The unconventional blade planform and twist distribution are the outcome of an optimization process which maximized the payload capability of the XV-15. Since the overall aircraft configuration precludes significant increases in cruise speed while large percentage increases in payload would result from small increases in hover thrust, the productivity index criterion led logically to the selection of blade parameters which matched peak hover efficiency with the maximum power available, while retaining the current level of high speed airplane cruise mode performance. This may be contrasted with the more familiar approach which would minimize fuel consumption (or maximize hover efficiency) at the design gross weight while maintaining an acceptable level of cruise efficiency.

The net outcome of the present process might be characterized as a blade with planform and airfoil distribution selected for hover capability and with twist selected to maintain cruise efficiency. Table I compares current metal blade and Advanced Technology Blade performance characteristics.

Other Objectives and Constraints

In addition to the performance and strength objectives, the blades had to be compatible with the existing aircraft in regard to dynamics and aeroelasticity, loads and handling qualities throughout the flight regime.

A requirement of the program was that strain gages and wiring should not compromise the aerodynamic contours of the blade. This led to the selection of a cured-in instrumentation package.

The twin pin retention was selected to facilitate interfacing with the XV-15 hub and potential future hubs. This design lends itself to limited variations of sweep angle , and this feature has become an important aspect of the design as discussed below.

Aeroelasticity

The aeroelastic behavior of tiltrotor aircraft is sensitive to many system design parameters including airframe stiffness and frequencies, mass distribution, rotor size, control system kinematics and the flexual and pitch/torsion frequencies of the blades. An adverse change in any one of these aeroelastically sensitive parameters will require compensatory changes in others to restore satisfactory stability margins.

The change from blades with a solidity of 0.089 to the ATB with solidity equal to 0.103, represents a major change in rotor aerodynamics. In addition, the increase in blade chord results in a significant increase in blade inertia about the pitch axis.

Stability analyses showed that this would reduce the critical speed to 337 knots at the design RPM for cruise, as shown in Figure 7. Stability up to 360 knots is required to meet the 1.2 V_D criterion. A solution had to be found within the new rotor system since aircraft modifications would have unacceptable cost and schedule impacts. The twin pin retention design provided such a solution since this lends itself to limited adjustments in blade sweep with respect to the feathering axis. At the large collective angles associated with high speed cruise, sweep becomes effectively a reduction in precone. This reduces the steady bending moments associated with the cruise loading of the blade and this in turn substantially reduces the lag-pitch coupling which is one of the mechanisms tending to destabilize the rotor-wing system. Introducing sweep outboard of the blade pitch bearings also adds aerodynamic stiffness and damping to the blade pitch degree of freedom. The introduction of one degree of sweep at the pitch housing blade junction restores adequate stability margins, as shown in Figure 7 and 8. The methodology of Reference 2 was used in these investigations of aeroelastic stability.

The effectiveness of introducing sweep is this manner was confirmed in wind tunnel tests of a dynamically similar 1/5 scale model of the wing and rotor. One degree of sweep has been selected as the baseline design and bushings for 0, ±0.5, ±1.0, ±1.5 degrees will be available for possible research investigations during the flight test program.

Tip and Cuff Variations

The tip cover is removable providing access to track and balance weights. This feature affords the opportunity to test alternate tip configurations. Similarly, the removable cuff configuration permits research on variations in cuff geometry. During the full scale hover test program conducted at the NASA Ames Outdoors Aeronautical Research Facility during the summer of 1984, two alternate tips and one alternate cuff were tested in addition to the basic design as indicated in Figure 9. The blades were also run at different sweep angles.

Development Procedures

Once the aerodynamic parameters have been defined, the development of a complex blade such as the XV-15 ATB becomes a coordinated effort which factors all the considerations of the relevant disciplines into the design.

The Dynamics and Structures activity proceeds from an analysis of rotor frequency placement requirements for the helicopter, transition and airplane flight modes. This determines the required mass and stiffness distributions and therefore the blade's structural material and cross section requirements over its length. Based on the associated dynamic loads, the blade's structural requirements are further analyzed and defined. This procedure is iterated until all requirements for frequency placements and strength have been met by the selected structural materials and cross sections.

The Materials and Processes organization defines the characteristics of state-of-the-art and advanced materials selected and establishes design requirements for use of these materials by notations on drawings and by issuance of manufacturing process documents. This is often accomplished by laboratory tests to verify the design approach and material selections in critical areas. In addition, the M & P and Structures staffs in conjunction with material manufacturers must establish the material structural properties, prepare material specifications, and qualify advanced materials for use in the blade. All material characteristics and properties are established by the M & P and Structures organizations through laboratory processing tests, and static and dynamic load coupon testing.

For example, early in the ATB program it became obvious that the graphite prepreg material currently used at Boeing Vertol would not be acceptable in the thick root laminate because of gaseous emissions during the cure. In the thick packs of graphite (0.30 inches/0.762 cm) used in the ATB root end straps and even more bulky fillers, this would cause unacceptable porosity and voids in the cured parts. There was a need to qualify a non-gaseous material and American Cyanamid's Celion 6000ST/Cycom 950 prepreg system, then becoming available, was selected. This material had the additional advantage of a significantly higher strain capability. Laboratory testing of this system demonstrated a 42 percent improvement in the allowable fatigue strain relative to the 250°F (121°C) curing T300 graphite epoxy system used in other applications at Boeing Vertol (Figure 10). This testing also demonstrated significant improvements in static strengths and improvements in stiffness properties.

Other development activities involve the Manufacturing Technology staff who determine appropriate tooling and assembly techniques to accurately and efficiently produce the required aerodynamic and structural characteristics of the blade. In the development of the design concept Manufacturing Technology engineers and blade designers work together to define construction features which will be compatible with tool designs and assembly techniques. This team effort results in a Master Layout of the blade assembly which is used to prepare the detailed design drawings, tool designs and manufacturing process documents.

Structural Description

Blade Assembly

The blade, shown in Figure 2, is composed of a structural assembly, a detachable aerodynamic root fairing (cuff) and a removable tip shell assembly, and incorporates a two-pin, four-lug, root attachment fitting or pitch change housing which interfaces with the XV-15 hub.

The tip cover is removable from 0.90R (90 percent radius) and provides access to the balance and tracking weights. The removable cuff extends from the spinner fairing to 0.30R. Since rotor hover performance is sensitive to variations in tip design, details such as taper, sweep and airfoil section and cruise performance is significantly affected by design parameters such as twist, planform, airfoil and camber over the inboard sections of the blade, the replaceable feature of these components provides the opportunity for full scale research on these performance sensitive variables.

The twin-pin clevis retention provides the opportunity for changes in parameters such as sweep, the aeroelastic significance of which has already been discussed. In addition, this configuration places very few restrictions on the design of any new hub system that might be adopted at a later time.

The twin pin, four lug blade retention system has additional merit in terms of fail safety because of the multiple load paths. This has been demonstrated on other Boeing Vertol designs. Structural testing of ATB specimens is discussed in a later paragraph.

Blade Structural Assembly

A cross section taken of the blade at 0.3R is shown in Figure 11. The Blade Structural Assembly consists of a D-spar (composed of unidirectional fiberglass and graphite epoxy straps, ±45 degrees biasplied fiberglass and graphite epoxy torsion wraps, unidirectional fiberglass epoxy nose block, and segmented steel balance weights), polyurethane and electroformed nickel erosion caps, aluminized fiberglass cloth and Nickel 200 lightning protection, ±45 degrees biasplied fiberglass epoxy fairing skins, Nomex honeycomb core and unidirectional fiberglass epoxy trailing edge wedge.

The major issue in selecting this mix of materials with different moduli was to provide appropriate blade physical properties relative to the metal XV-15 blade and its natural frequencies and strength. The Advanced Technology Blade is designed to place natural frequencies at values acceptable to the XV-15 aircraft and to provide strength and blade life which meets or exceeds design criteria. Table 2 presents the materials and pertinent properties relative to the blade element for which it is used.

Root End Design

As shown in Figure 12, the spar configuration employs a two-pin, four-lug, root wraparound retention system. The attachment pin holes are lined with filament wound fiberglass sleeves. Figure 13 shows the spar strap orientation at an intermediate station between 0.17R and 0.30R. In the ATB, this change in spar strap orientation was made over a shorter distance than previously attempted. Figure 13 also shows the variable section filler parts which are required as the straps transition from vertical loops at the pins to become the upper and lower caps for the spar at 0.30R.

Tip Weight Fitting Design

As shown in Figure 14, at the outboard end of the spar, unidirectional fiberglass wraps around the tip weight fitting to provide CF retention. Sufficient teeter balance and tracking weight capacity and adjustment capability is provided for the normal weight, span moment and product moment variation expected in manufacturing. Nominally, there is 3.5 pounds (1.6 kilograms) of span balance weight and 1.4 pounds (0.64 kilograms) of tracking adjustment weight. There is an additional span balance capability for fine tuning (without removing the tip covers) using weight pockets under the tip section retention screws at 0.87R. Up to 30 gms adjustment is available.

Tip Shell Assembly

The removable fiberglass tip shell assembly has an elliptical planform over the outboard 10 percent of the blade span. The aft fairing is a Nomex honeycomb sandwich structure; the tip shell spar is unidirectional fiberglass; the skins are biasply (±45 degrees) fiberglass; the erosion cap is electroformed nickel. The tip shell assembly is readily removable allowing access to the tip weights for balance adjustment.

Erosion Protection

Erosion protection of the leading edge of a composite blade is important. Polyurethane is used over the major portion of the blade because of its low cost and resistance to erosion in sand and dust. It is also replaceable without damage to the blade subsurface. From 0.69R to the tip an electroformed nickel cap is used for erosion protection.

In a sand and dust environment polyurethane is more resistant to erosion than metal. However, at impact speeds in excess of 450 ft/sec (137 meters/sec), it becomes vulnerable to erosion by large rain drops. The outboard limit of the polyurethane is where the blade helical velocity is in the threshold area of rain erosion vulnerability. It is also where the outboard blade contour and planform geometry begins to vary. Thus over the outboard 31 percent radius of the blade, nickel offers superior erosion protection. In addition, electroforming nickel is a logical manufacturing method to use in this area of varying blade leading edge contour, planform taper and very sharp leading edge radii.

Instrumentation

The ATB instrumentation installation is believed to be a major improvement over previous practice. The approach is based on techniques developed and proven over recent years in rotor test programs in the Boeing Vertol Wind Tunnel. The ATB gages are laid on the surface of shallow depressions molded into the precured spar at predetermined locations. The gage wiring is routed chordwise in depressed shallow troughs to the rear of the spar heel and then radially along the neutral axis of the blade. The gages and chordwise wiring are covered with insulating and protective outer layers of materials, such as adhesive films and fiberglass skins, which are laid up and cured over the gages and wiring at the same time that the aft fairing is bonded onto the spar. This encapsulation of the gages and wiring,

along with the location of spanwise wires in a minimum strain environment, practically eliminates wiring and solder joint failures.

In wind tunnel tests of model scale rotor blades exploring higher strain situations and with a much higher rate of accumulation of alternating loads than full scale, instrumentation of this type has been found to last at least five times as long as when externally attached. Typically, gage life exceeds one million cycles at alternating strain levels of 1,500 micro in/in.

In addition to the extended life of the instrumentation system, this approach permits an uninterrupted blade surface finish with no bumps, indentations, or channels to adversely affect aerodynamic performance. The successful demonstration of this instrumentation approach in a full scale application will be a significant advance in the state-of-the-art.

Tooling and Fabrication

The manufacturing processes for rectangular composite helicopter blades are well established. However, the development of processes and tooling for the non uniform tapered, highly twisted ATB presented a significant challenge. This was met using NC (numerically controlled) machined matched metal molds which were segmented for versatility so that the same tools could be used in different phases of fabrication and assembly as shown schematically in Figure 15. The blade spar was precured using the front segment of the mold with a closure at the spar heel location. The spar was inspected and instrumented before the bonding of the honeycomb core and aft fairing using the full-chord mold shown in Figure 16. For the cuff fairing, where dimensional tolerances were not so critical, wooden patterns were used to produce composite molds with metallic flame sprayed surfaces. The integration of the design and tooling activities was facilitated by the use of the Gerber Interactive Design System (IDS). This defined the aerodynamic contours at control stations an inch apart over the length of the blade. Transition contours from the rectangular cross sections near the root to the VR7 airfoil at 0.30R and to the VR8 airfoil at 0.95R were generated by an automatic lofting feature of the IDS, which also automatically generates twisted contours from the section properties and twist schedules. The system then generates Master Dimensioning Identifiers (MDI) which are processed to provide a code for the machine tool which cuts the molds.

The IDS was also utilized to define spar strap tape paths, mold lines for filler layups, flat patterns for torsion wrap layers and skins, cross sectional areas of elements for ply count determinations, aft fairing core contour MDI, electroformed nickel erosion cap mandrel MDI, outboard spar extension and tip cover support rib mold MDI, and spar heel mold MDI.

The Production Automated Tape Layup Machine (PATLM), shown in Figure 17, was used to layup the unidirectional fiberglass and graphite spar straps. The biasplied fiberglass and graphite components such as spar torsion wrap and skin layers were cut out of biasplied broadgoods using the NC Gerber cutter, shown in Figure 18.

The Nomex honeycomb core was designed to be NC contour machined on the upper surface only, in the untwisted flat position; the MDI defining the

upper contour were mathematically developed to compensate for the lower contour.

The IDS also generated dimensional data for machining the mandrel used to electroform the nickel cap for the outboard sections of the blade. The actual electroplating was subcontracted to a house specializing in such work.

In summary, many of the traditional steps in the tooling and fabrication process were replaced by computer operations which translated the wishes of the designer into operations on the shop floor such as automated tape layups, computer controlled cutout of broadgoods, and NC machining of the steel bonding assembly jigs. This resulted in significant cost savings and improvements in quality control.

Structural Testing

Static strength, stiffness, deflection and natural frequency tests were performed on each blade. No significant variations were noted between blades and properties established by test agreed well with the design objective and predicted values.

Fatigue testing is reviewed in more detail; the fatigue strength of an unconventional blade with mixed modulus material is less predictable than the other structural properties.

At the root end, all blade loads are transferred from the composite spar strap loops to the metal hub through a interface consisting of retention pins and a steel clevis - pitch housing assembly. The composite part of the root is designed by stiffness considerations and was predicted to have much higher margins of safety than the metal parts which, because of the high modulus of steel, were designed for strength. However, the composite root end had a number of unusual features which went beyond previous experience. For example, the spar straps are rotated from the vertical pin orientation to conform with the upper and lower blade surface in a shorter percentage of the span than previously attempted in helicopter practice. This was to achieve the 12 percent thick VR7 airfoil section as quickly as possible. This required rapid material drop-off in root end fillers and estimated bond line stresses were higher than previous experience. In addition, there is no lag hinge and the blade droop stop structure experiences fatigue loading when the retention alternating loads exceed steady centrifugal forces. This had not been encountered with the same severity in helicopter applications. The highest loads in the root end occur around tilt angles of 60 degrees in the transition mode of operation.

Design loads for the outer blade occur when the aircraft is flown at maximum speed in the helicopter mode and higher frequency blade modes are excited by the aerodynamic forces. This modal response increases the bending moments over the outer radial sections of the blade, where blade strength and stiffness is reducing rapidly. In the ATB the highest stresses are predicted around 65 percent radius, where the final drop-off of unidirectional graphite causes a discontinuity in stiffness and a stress concentration. These factors made it essential that the fatigue strength of the outer blade be validated by test.

The helicopter mode at high speed is also critical for the tip region. Bench test validation of the tip weight retention and tip shell retention using metal screw fastening was essential. The test program on the tip assembly included fatigue testing for flight loads, ground-air-ground cycling of centrifugal loads and an investigation of high temperature effects which might result from desert operations.

Expanded Transition Envelope

Figure 19 shows the XV-15 design transition envelope in terms of rotor tilt angle versus speed, along with the limitations imposed by the strength of the original steel blades; also shown are the limits, based on fatigue test results, for the Advanced Technology Blades. The ATB limits indicate that the full design transition envelope may be flown and that there is margin for maneuvers at the envelope speeds.

Root End Testing

Initial testing of the root end specimens disclosed deficiencies in the design of retention pin nuts. These were redesigned in a different alloy to eliminate galling, and additional material was added in critical areas. Testing proceeded and the most heavily loaded lug of the pitch housing failed first as expected. This occurred at 800,000 cycles at 180 percent of design loads after run-outs had been experienced at 150 percent load levels. The intact composite part of the root ends were then mounted in an over strength dummy clevis and testing continued until failure of the droop stop occurred.

Failure of both root end components is considered fail-safe since the system could still sustain normal flight loads.

Outer Span Test

The specimens were tested to 10 million cycles at 150 percent of design loads, thus substantiating the adequacy of the design. Attempts were made to fail the specimens by raising the loads but this was terminated because of rig fixture failures.

Tip Specimen Tests

The specimens were tested to 10 million cycles at 150 percent of design loads without incident. Because of the removable tip shell design, separate centrifugal force loadings were applied through the tip cover and through the tip weight fitting structure.

Following runouts at the initial load levels the specimens were subjected to 15,000 cycles of ground-air-ground centrifugal force loading.

The bending moments on the first specimens were then raised 25 percent and testing continued. A gradual increase in deflection was noted. After 9 million cycles at the higher loads, deflections increased rapidly and a failure was declared. Figure 20 shows the fail-soft character of the structural degradation.

The second specimen was subjected to an additional 7500 cycles of ground-air-ground loading with the blade upper surface temperature raised to 180°F (82°C) to simulate solar heating in the desert. A increase in deflections was noted around 3000 cycles and post-test inspection indicated damage to the blade spar at the fastener inserts for the outer row of screws. Standard repair procedures were applied and the specimen was subjected to additional dynamic loading with bending moments increased 60 percent. At this load level, the deflections began to grow and the test ended after 34,000 cycles when the rig could no longer apply the deflections required to maintain the loads.

The test program demonstrates that blade strength will not be a factor limiting the operation of the aircraft. During the flight program the test data will be used with measured flight loads to define a flight spectrum consistent with a 3000 hour life for the blades.

Aerodynamic Testing

Test Objectives and Rationale

An important program objective was to obtain reliable data on isolated rotor performance. At the inception of the program, the overall performance in hover of the XV-15 aircraft with steel blades was known from flight test. However, the degree to which rotor thrust was negated by wing down-load was not known. An earlier test of the XV-15 steel blades on a whirl tower at Wright Patterson Air Force Base (Reference 3) was thought to be compromised by aerodynamic blockage of the support structure. Performance estimates had been made accounting for this blockage and these in turn were used with the observed aircraft performance to estimate down-load effects. It was therefore important to establish definitive isolated rotor performance data for the XV-15 steel blades and the ATB's, not only to evaluate the relative merit of the two, but also to establish the performance decrement due to down-load in the XV-15.

The present test has established that rotor performance is significantly better than previously believed with the corollary that download must be worse.

Development of Test Facility

A planning survey disclosed unacceptable deficiencies in all the available rotor test facilities, and a crash program was initiated, as part of the ATB contract, to upgrade the rig used at Ames Research Center for full scale rotor and propeller testing. New hardware developed included a 4:1 reduction gear box to match the HP/RPM requirements of the test. A new balance was developed for accurate and direct measurement of rotor thrust and torque with minimal interaction from the other loads. This design, shown schematically in Figure 21, virtually eliminates the problem of thermal drift. It also accounts for the effect on primary thrust measurements of the stiffness of the flexible couplings in the drive shaft and for power losses due to friction in the bearings between the rotor and the primary torque measurement at the flexible couplings. Periodic check loadings demonstrated that the installed system was accurate to 0.3 percent of maximum thrust and 0.3 percent of maximum torque. Figure 22 is an exploded view of the installation.

Figure 23 shows the ATB installed on the test rig at the Outdoors Aeronautical Research Facility (OARF) at Ames Research Center. The rotor center is 1.76 radii above the ground and the support structure is designed to minimize blockage. The rake for sensing wake velocity and distribution is visible but microphone installations are in the stowed position in this photograph.

Hover Performance Results

The Advanced Technology Blades were tested in series with the XV-15 steel blades and a set of blades scaled to represent the V-22 rotor system. Aspects of the XV-15 and ATB tests will be discussed here. An account of the hover testing of all three configurations is given in Reference 4. The V-22 test program included down-load investigations using a simulated wing and this is reported in Reference 5.

All the rotor systems tested achieved higher peak figures of merit than predicted by contemporary theory. It was also observed that figure of merit remained high up to the point of rotor stall. The XV-15 rotor attained a peak value of 0.79 at a C_T/σ of 0.12. The ATB demonstrated a value of 0.80 at a C_T/σ of 0.165. These figures of merit are significantly higher than those of typical helicopter rotor systems due to the higher twist and higher disc loadings of the tiltrotor configuration.

In addition to accurate measurement of rotor performance the test provided background data on tip vortex geometry, wake contraction and downwash velocity distribution. These are providing an empirical basis for improvements in performance methodology.

Figure 24 shows a typical plot of C_T versus C_P for the ATB rotor. The data showed little scatter and was repeatable. Figure of merit was evaluated based on mean lines faired through such data for the XV-15 rotor and the ATB rotor. As shown in Figure 25, the ATB performance peaks at a higher value of C_T/σ than that of the XV-15.

The current XV-15 blades cannot exceed a C_T value of 0.016 because of a rapid rise in vibratory blade and control loads. The ATB demonstrated a C_T of 0.0215, the rotor maximum, before such load rise phenomena were encountered. This may be attributed to the thinner airfoils and tapered planform of the ATB. These factors also account for the increase in ATB figure of merit in spite of the 12 percent increase in solidity. At transition RPM the difference in rotor thrust capacity is equivalent to an approximate increase of 0.5g in maneuvering load factor at the nominal gross weight of 13,000 pounds (5897 kilograms).

Figure 9 shows the array of alternate tip and cuff configuration tested. The airfoil of the baseline cuff is truncated, as required for adequate clearance with the XV-15 airframe when the rotor is at high collectives and the nacelle is on the cruise position. The impact of the truncation was investigated by testing a full chord cuff; in addition, data was taken with the cuff removed. The results are shown in Figure 26. There is an increase in peak figure of merit from 0.80 to 0.81 when the cuff trailing edge is extended; with the cuff removed there is a reduction to 0.77.

Figure 27 shows the effect on ATB performance of change in tip configuration. The square tip has an adverse effect on performance as expected, and the swept tip improves figure of merit at the lower C_T values. This is not understood, since the Mach number at the elliptical tip is well below that of drag divergence. A possible explanation may be that the pitching moment due to the swept tip causes sufficient torsional deflection over the length of the blade to affect performance.

Downwash Velocity Distribution

Figures 28 and 29 show typical velocity distribution in the wake of the XV-15 and ATB rotors respectively. The downwash velocities are shown for two thrust coefficients, 0.008 and 0.014. Both rotors show an outward shift of maximum wake velocity as thrust increases. At the higher thrust condition, where the XV-15 rotor requires more power than the ATB, the XV-15 wake is less uniform, as might be expected from theory.

Wake Geometry

More than 60 photographs were taken of the rotor tip vortex condensation trails, generated at values of C_T/σ greater than 0.16. The thrust and torque for each photograph were recorded. Figure 30 shows one such photograph. The photographs were analyzed to provide estimates of wake velocity and wake contraction. Data for the position of the condensation vortex aft of the rotor disc are shown in Figure 31 for a typical high thrust condition. The mean line through these points is compared with those calculated using Landgrebe's and Kocurek's methods (References 6 and 7). It is noted that both methods indicate constant velocity until the passage of the first blade following the generating blade, while the test data indicates continuous change.

Wake contraction data is shown in Figure 33. The mean empirical contraction is compared with calculated values in Figure 34, showing that the wake contracts more than the asymptotic value of 0.78 predicted by theory.

The methods of References 6 and 7 were developed for rotors with moderate linear twist, no taper and low disc loadings; also, in the Kocurek application, the "generalized" approach was used with a truncated iteration procedure. The data generated by this test program provides an empirical basis for extension of these methods to highly twisted, tapered, rotors operating at high disc loading.

However, corrections to the wake geometry may not be sufficient to provide accurate performance predictive capability. Figure 35 compares measured ATB performance with that calculated using the Kocurek and Landgrebe wake definitions. One point was calculated using the observed wake at C_T/σ = 0.17. Even with the experimental wake, the calculated figure of merit falls short of the measured value. Thus the errors at high thrust coefficients are not solely due to errors in the assumed wake geometry. The rapid drop in calculated performance at high thrusts, while the measured performance remains high, would suggest errors in the mathematical modeling of airfoil stall.

Acoustic Testing

Near-field and far-field noise levels were measured during the hover test program. The near-field microphone position represented a point on the side of the fuselage of a typical tiltrotor in hover. Far-field noise was recorded with an array of microphones at 250 ft (76m) and 650 ft (198m) radius at 0, 15, 30, and 45 degrees behind the rotor disc. Near-field and typical far-field OASPL's (overall sound forward level) are presented as a function of rotor thrust in Figures 36 and 37. At the higher thrust levels the ATB near-field noise level is approximately 2-3 dB less than the noise level of the XV-15, and the far-field OASPL is approximately 5-6 dB lower. These comparative noise levels trends are to be expected since the tip pressure loading is less for the tapered, higher solidity ATB with its more even spanwise distribution of thrust.

The data acquired in these isolated rotor tests will be of value in calibrating prediction methods and, along with the measured XV-15 noise levels, can be used to estimate the effect of airframe interactions on internal and external noise.

Concluding Remarks

Thus far, the Advanced Technology Blade Program is noteworthy for successful accomplishments in a number of different categories. These include the achievement and demonstration of primary strength and performance goals, the application of innovative design and instrumentation concepts, extensive computer usage in the tooling and manufacturing process, successful fabrication of tapered highly twisted blades, and the acquisition of a unique base of large scale aerodynamic and acoustic data for tiltrotor systems.

With the Advanced Technology Blades the XV-15 aircraft will operate at higher gross weights and at higher altitudes than were previously possible, and operations in the transition mode will not be limited by blade strength considerations.

The extensive use of graphite in primary structure and other innovative design features have been demonstrated to be viable by ground test programs. The cured-in instrumentation has survived the hover test program which included hours of endurance running with representative alternating loads.

The computer integration of design, tooling and fabrication, initiated on the ATB program has now become standard at Boeing Vertol.

The accurate aerodynamic and acoustic data, generated by the hover test, constitutes a valuable resource for the guidance and evaluation of new developments in methodology. It is also noted that the definitive quality of the performance data may be credited to the balance system which was designed and fabricated as part of the ATB program. The benefits of this system will also be felt in future rotor test programs.

Other innovations included the introduction of blade sweep for aeroelastic stability. This will be evaluated during the flight test program which will commence in the Fall of 1985.

REFERENCES

1. McVeigh, M. A., Rosenstein, H., and McHugh, F. J., Aerodynamic Design of the XV-15 Advanced Composite Tilt Rotor Blade, paper presented at the 39th Annual National AHS Forum, May 1983.

2. Johnson, W., A Comprehensive Analytical Model of Rotorcraft Aerodynamics and Dynamics, NASA TM-81182, Part I; TM-81183, Part II; and TM-81184, Part III, June 1980.

3. Helf, S., Broman, E., and Charles, B., Full Scale Hover Test of a 25-Foot Tilt Rotor, NASA CR 114626, May 1973.

4. Felker, F. F., Maisel, M. D., and Betzina, M. D., Full Scale Tilt Rotor Hover Performance, paper presented at the 41st Annual National AHS Forum, May 1985.

5. McVeigh, M. A., The V-22 Tilt Rotor Large-Scale Rotor Performance/Wing Download Test and Comparison with Theory, paper presented at the Eleventh European Rotorcraft Forum, London, U. K., September 1984.

6. Langrebe, A. J., An Analytical and Experimental Investigation of Helicopter Rotor Performance and Wake Geometry Characteristics, USAAMRDL Report 71-24, June 1971.

7. Kocurek, J. D. and Tangler, J. L., Prescribed Wake Lifting Surface Hover Performance Analysis, paper presented at the 32nd Annual National AHS Forum, May 1976.

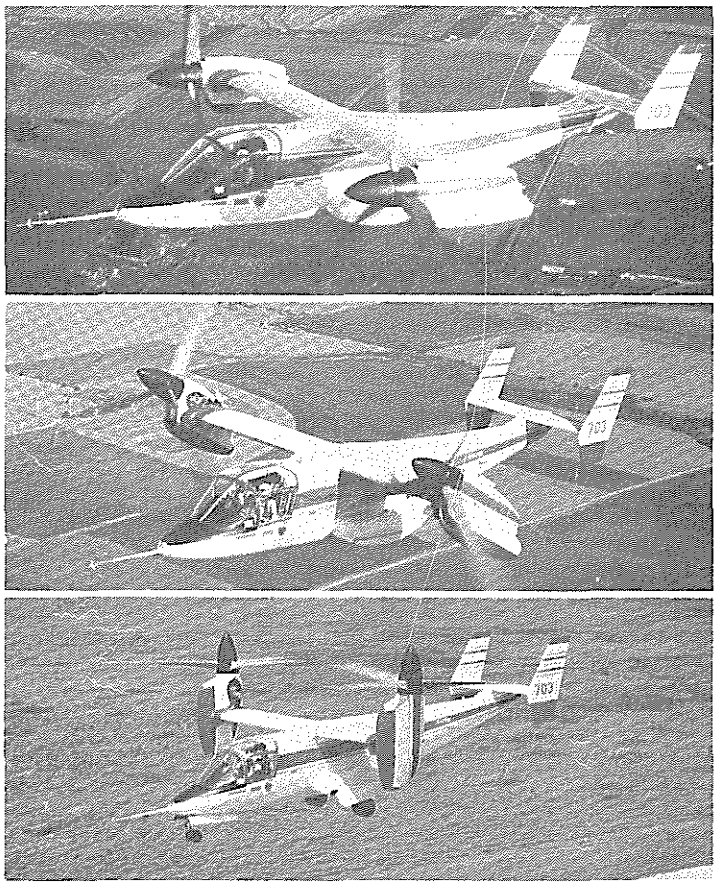

Figure 1. XV-15

Tiltrotor Research Aircraft

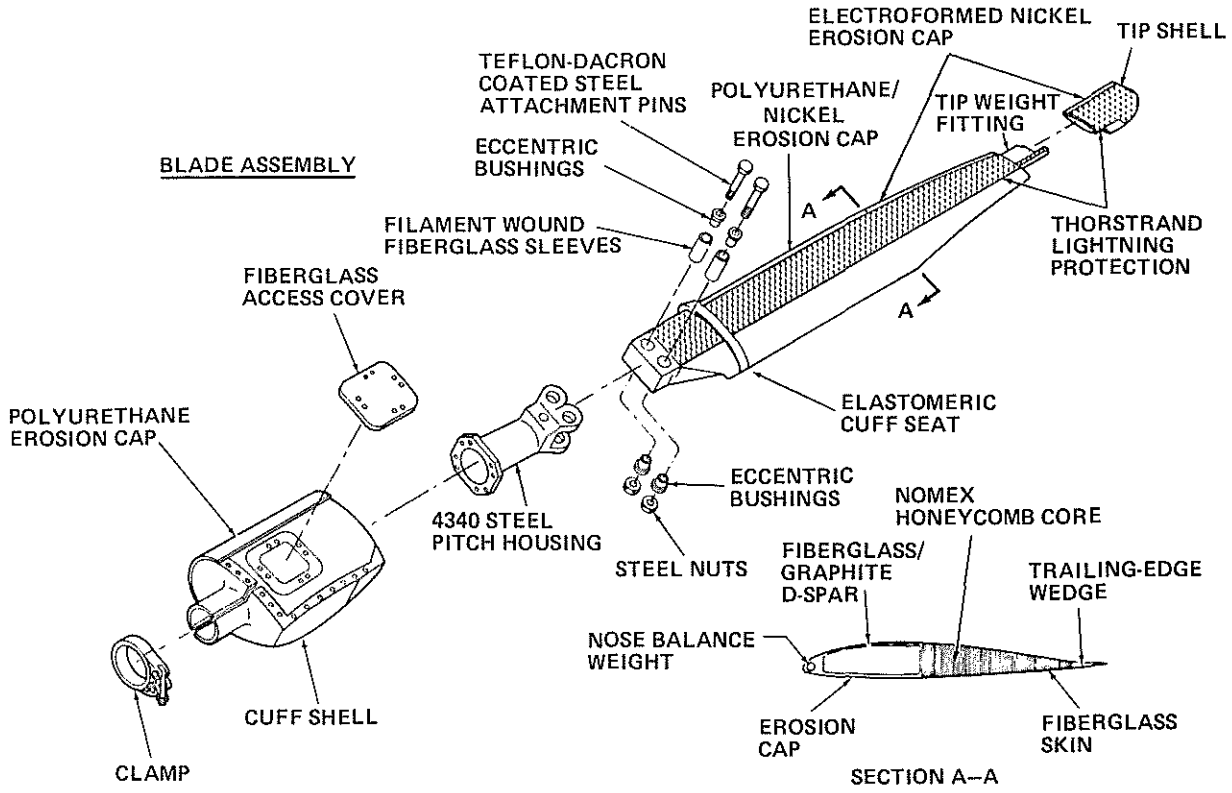

Figure 2. Advanced Technology Blade for XV-15

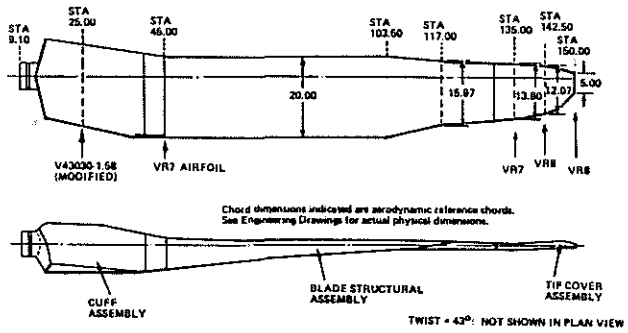

Figure 3. XV-15 Advanced Technology Blade Aerodynamic Definition

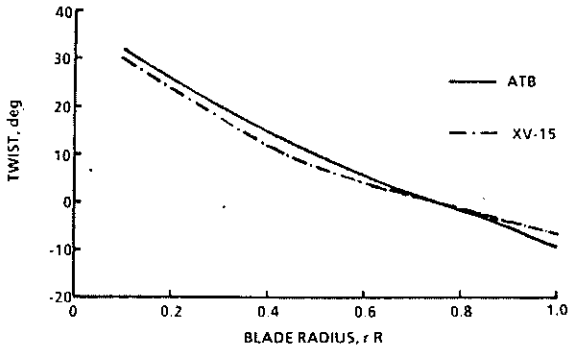

Figure 4. Blade Twist Distributions

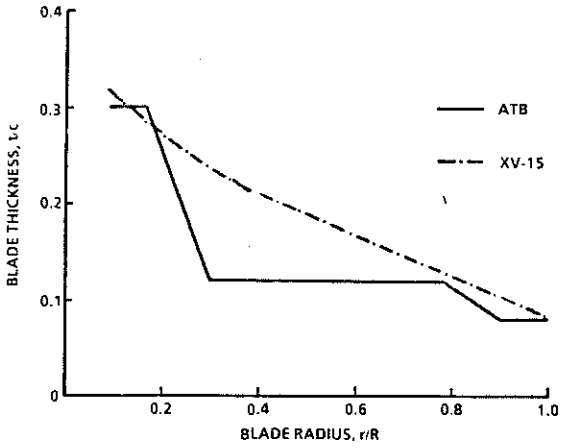

Figure 5. Blade Thickness Distributions

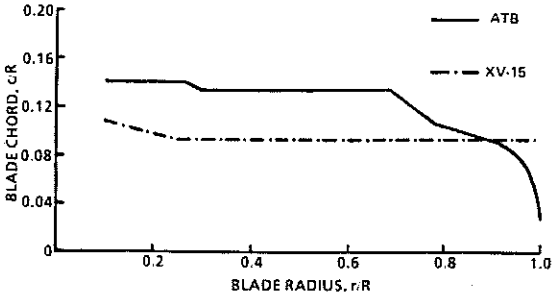

Figure 6. Blade Chord Distributions

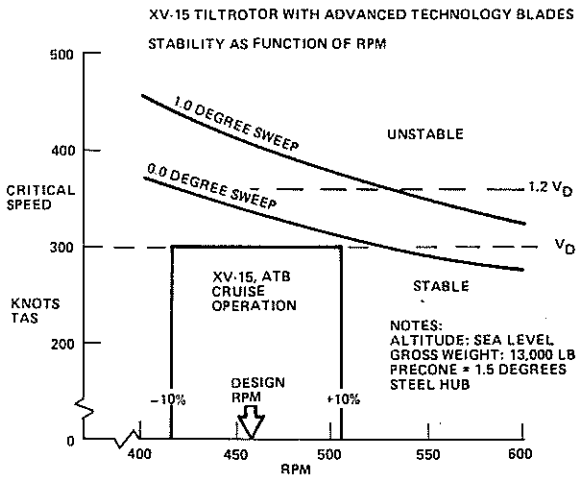

Figure 7. Stability of XV-15 With ATB 0.0 and 1.0 Degree Sweep

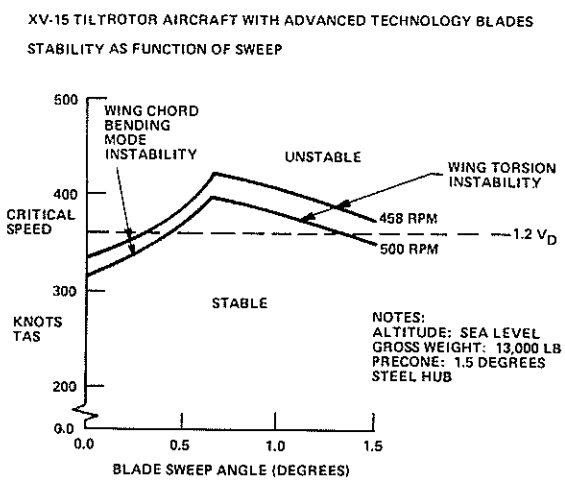

Figure 8. Aeroelastic Effect of Blade Sweep

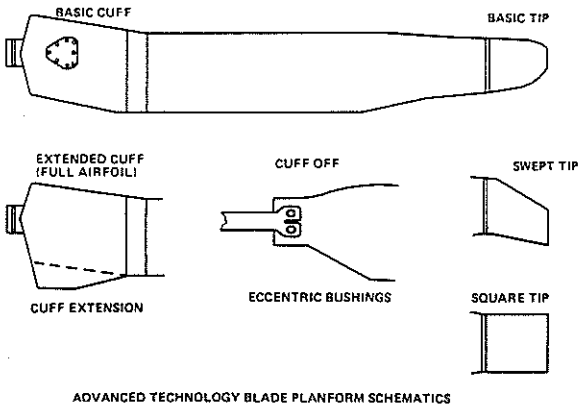

Figure 9. ATB Baseline Planform and Alternate Configuration

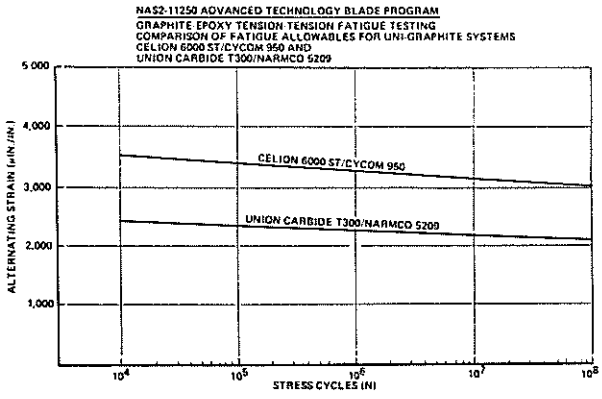

Figure 10. Tension Strain Allowables Established for High Strain Celion 6000 St/Cycom 950 Graphite Epoxy System

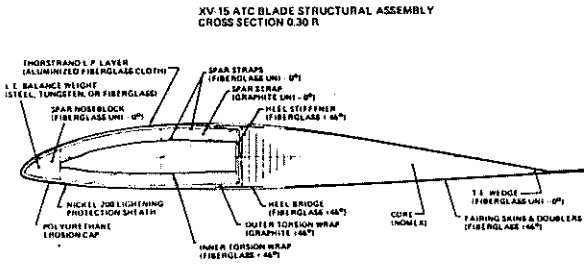

Figure 11. XV-15 ATB Cross-Section at 0.3 R

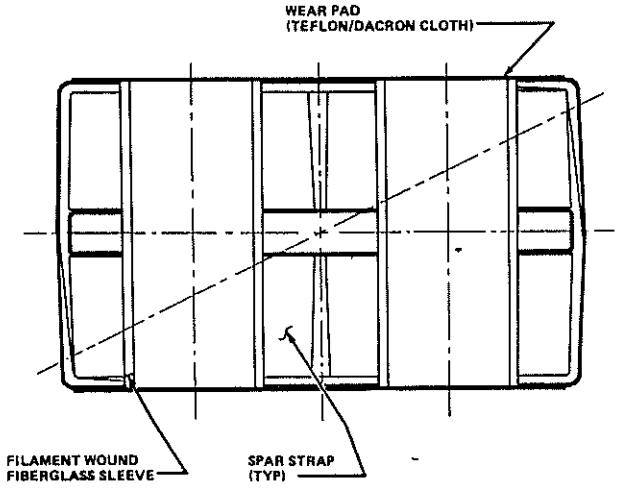

Figure 12. Blade Spar Cross Section at 0.17 R

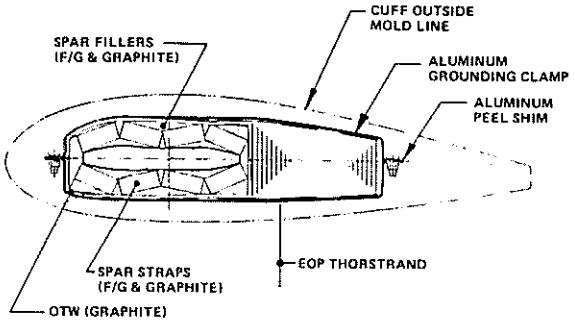

Figure 13. Cross Section at 0.23 R (Illustrating the Rotation of Spar Straps)

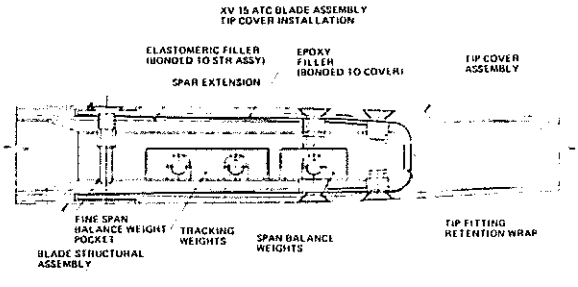

Figure 14. Spanwise Cross Section at Top Fitting

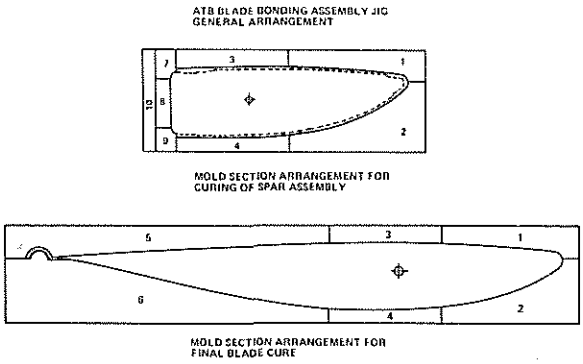

Figure 15. Tooling Concept for Bonding Assembly Jigs

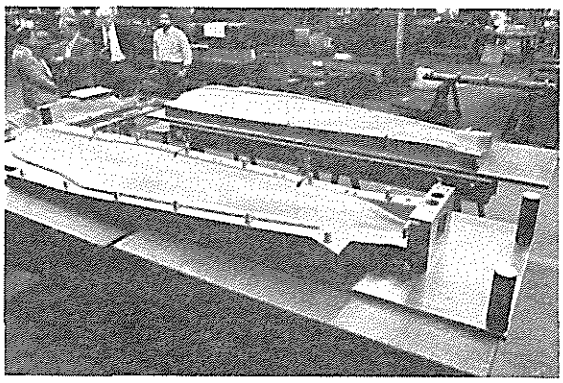

Figure 16. XV-15 ATB Main Bond Assembly Jig

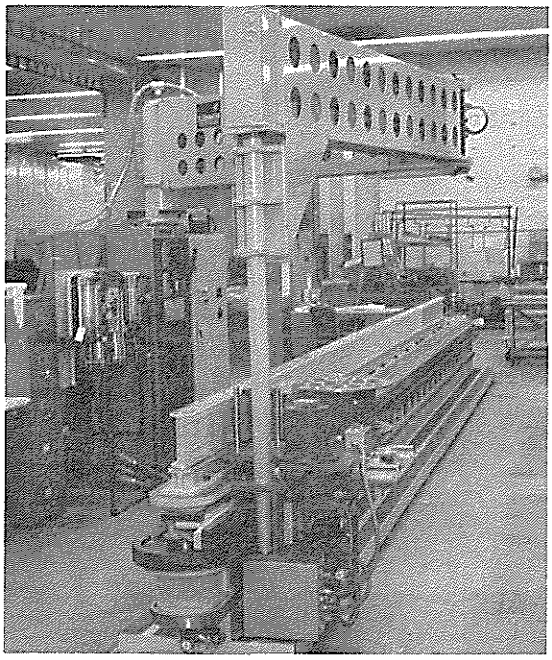

Figure 17. Spar Strap Layup on Production Automated Tape Layup Machine

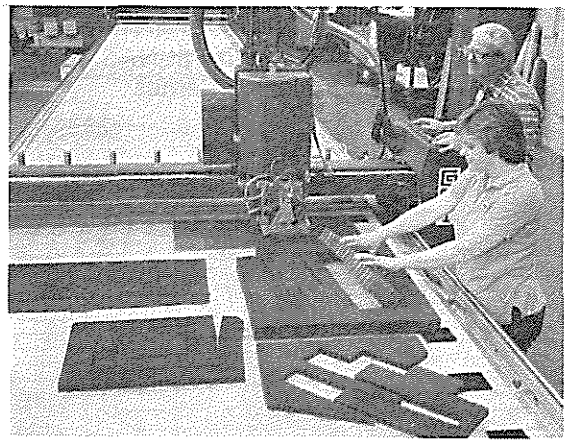

Figure 18. Gerbert NC Flat Pattern Cutter

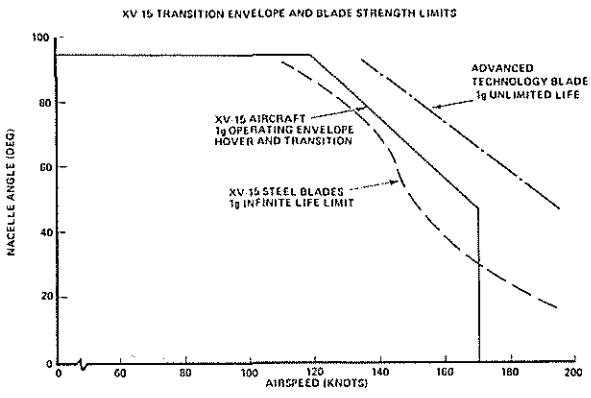

Figure 19. Expansion of XV-15 Transition Envelope With Advanced Technology Blades

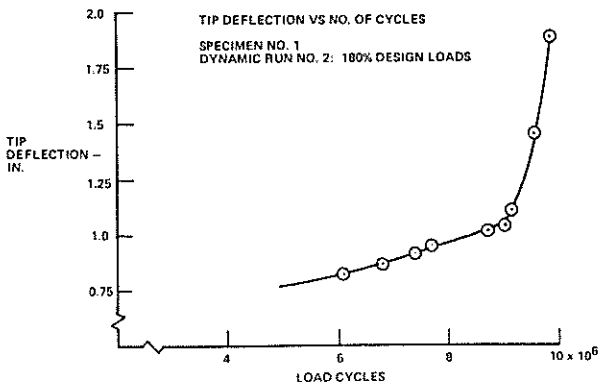

Figure 20. Soft Failure Characteristics of Composite Tip Specimen

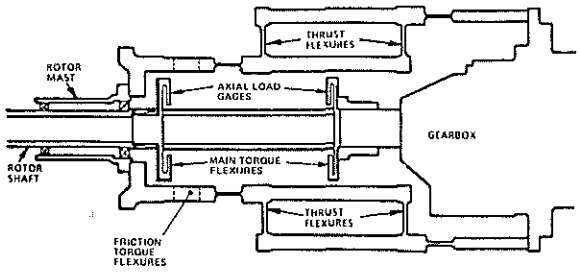

Figure 21. Schematic of Balance System

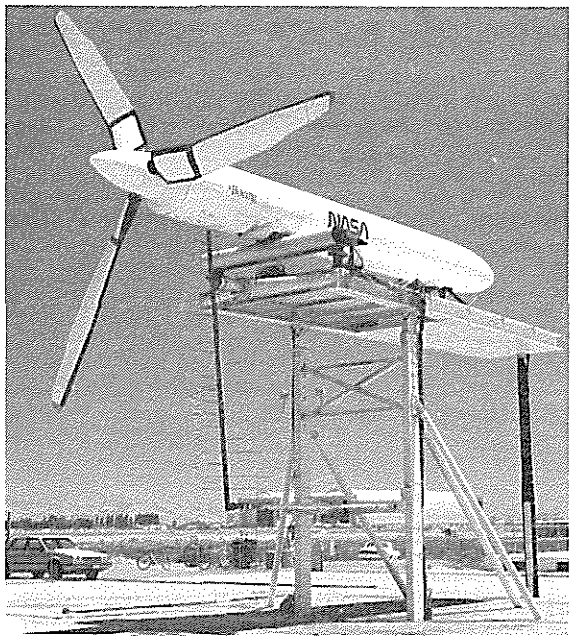

Figure 23. XV-15 ATC Blade Hover Test Setup at Outdoor Aeronautical Research Facility at NASA Ames Research Center

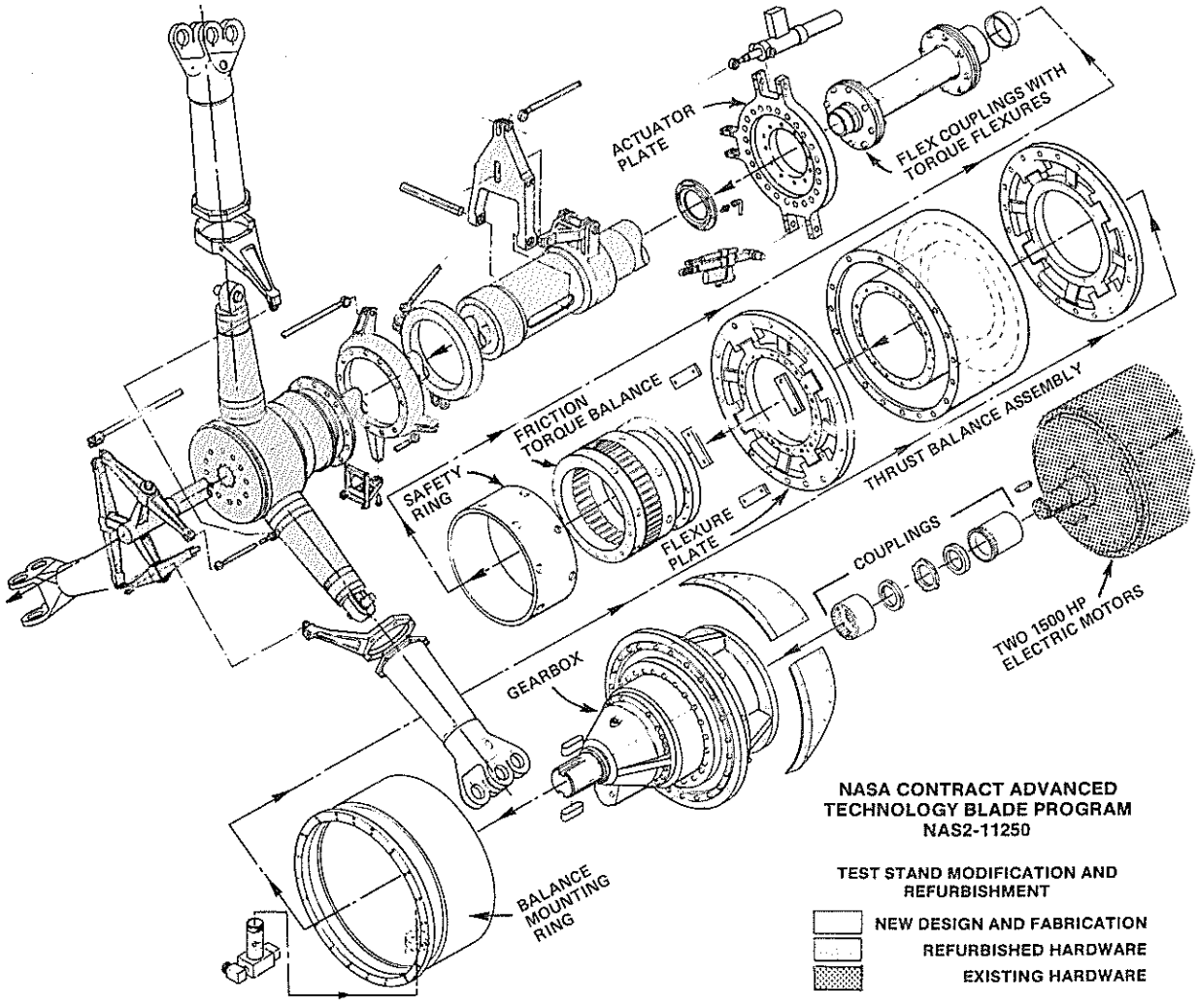

Figure 22. Test Stand Modification and Refurbishment

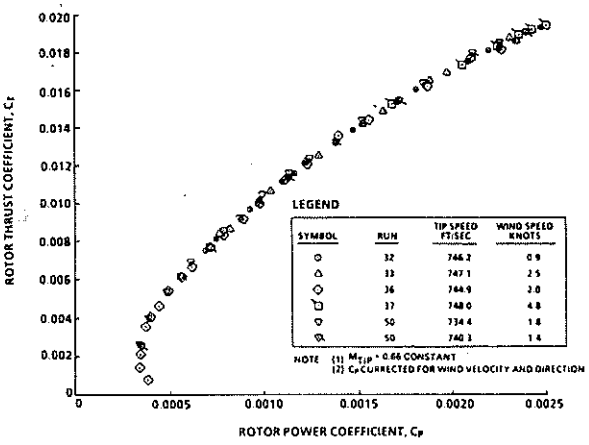

Figure 24. Thrust vs Power Coefficients for ATB Rotor (Baseline Tip and Cuff)

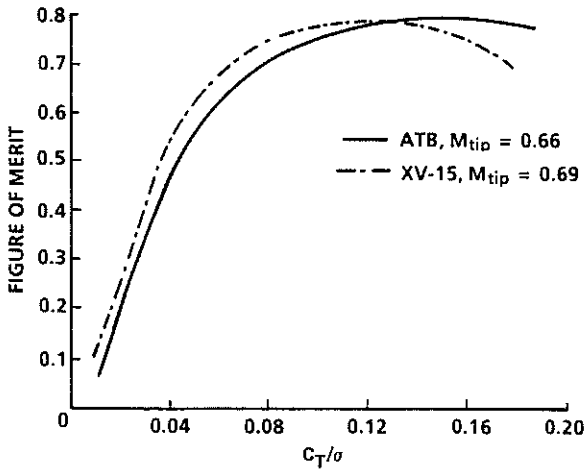

Figure 25. Isolated Rotor Performance

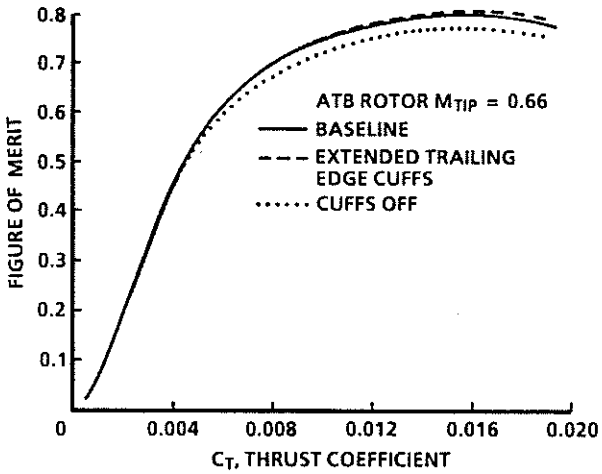

Figure 26. Effect of Blade Root Configuration Changes on ATB Performance

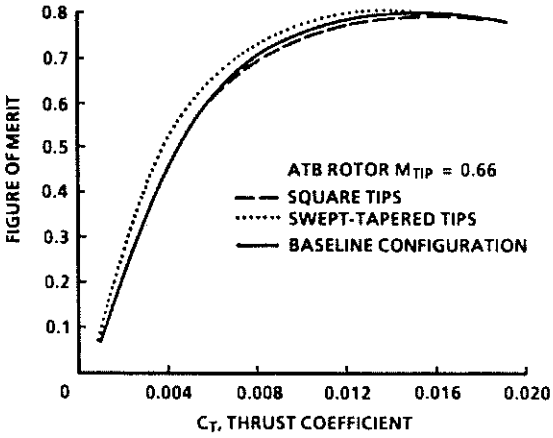

Figure 27. Effect of Blade Tip Configuration Changes on ATB Performance (With Extended Trailing Edge Cuffs)

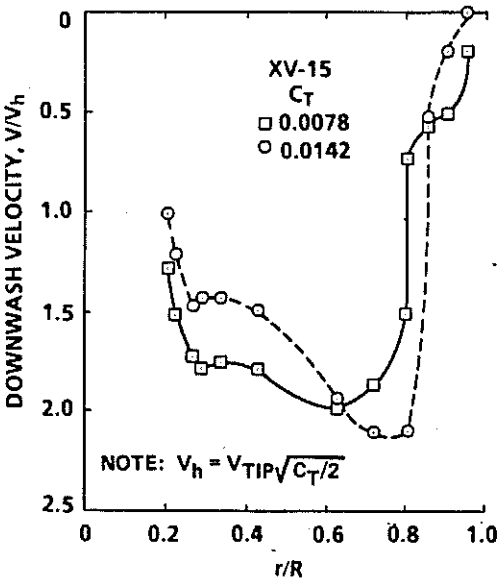

Figure 28. XV-15 Downwash Velocity

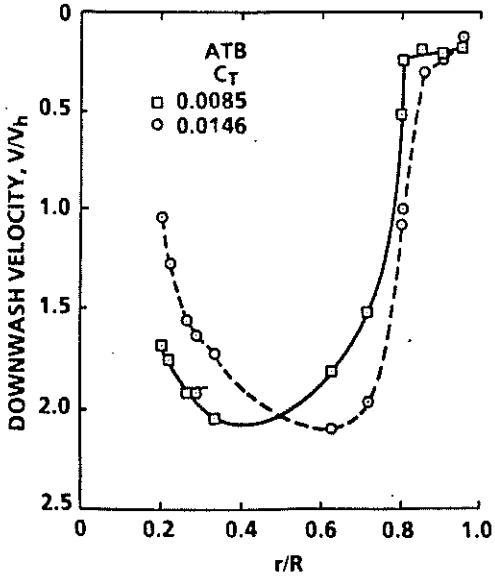

Figure 29. ATB Downwash Velocity

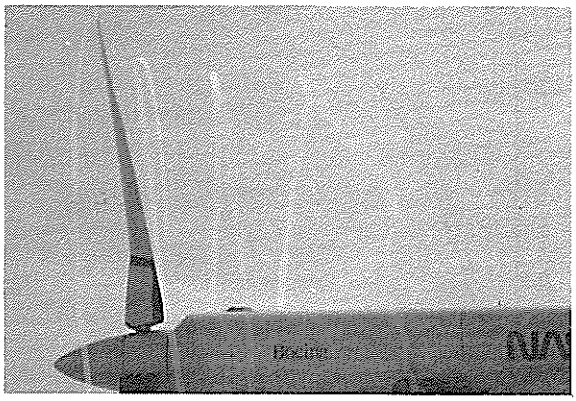

Figure 30. Rotor Tip Vortex Condensation Trail

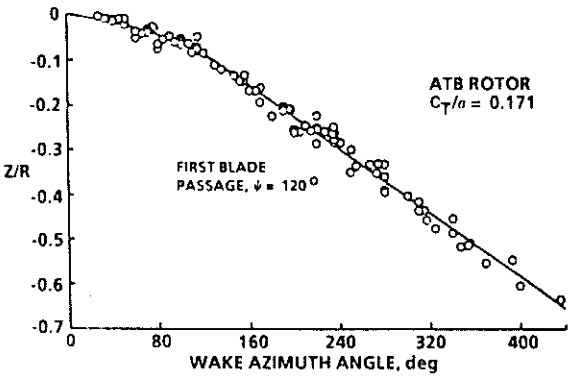

Figure 31. Typical Tip Vortex Position Data

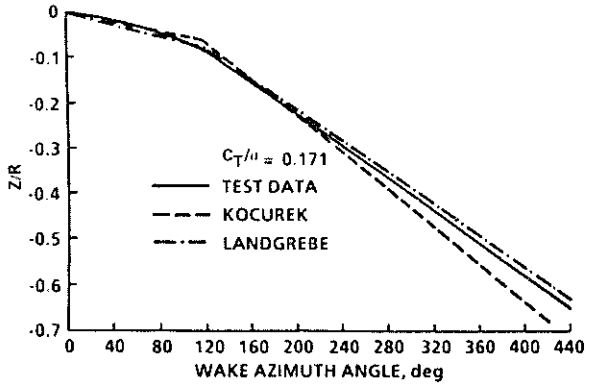

Figure 32. Comparison of Predicted Wake Geometry With Test Data

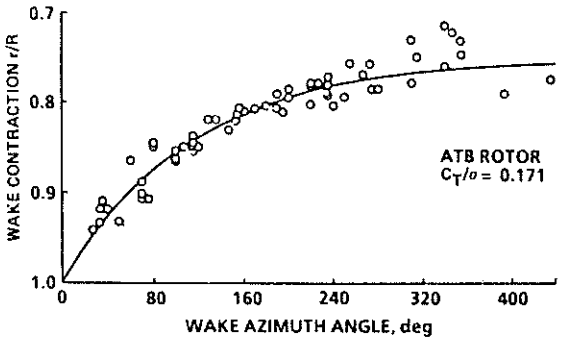

Figure 33. Typical Tip Vortex Geometry Data

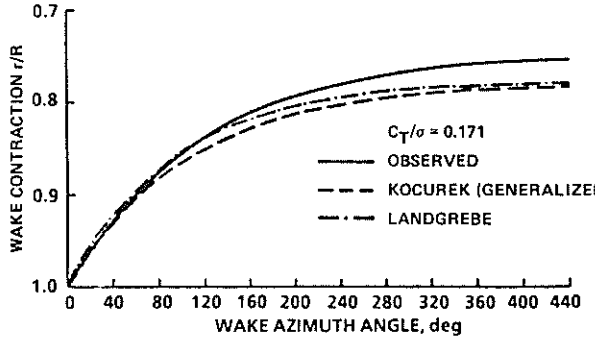

Figure 34. Comparison of Predicted Wake Geometry With Test Data

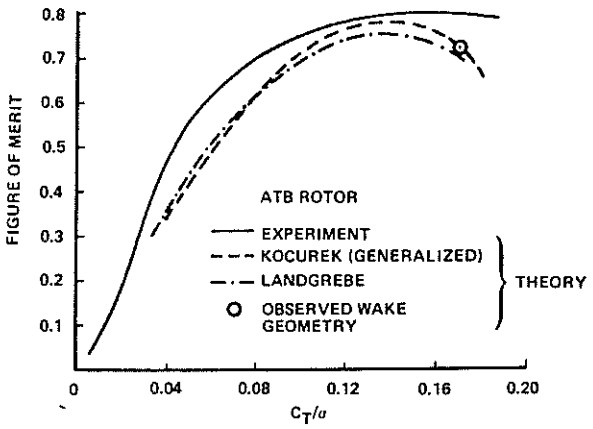

Figure 35. Comparison of Predicted Rotor Performance With Test Data

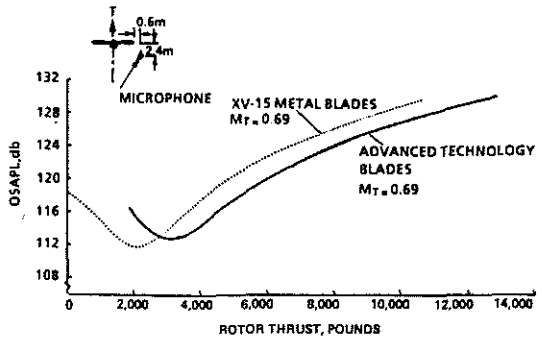

Figure 36. Near-Field Noise Data

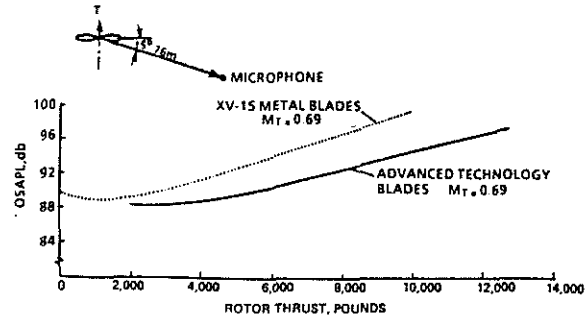

Figure 37. Typical Far-Field Noise Data

TABLE 1. XV-15 PERFORMANCE COMPARISON: CURRENT METAL BLADES VS ADVANCED TECHNOLOGY BLADES

PERFORMANCE VARIABLE	CURRENT XV-15 METAL BLADES	ADVANCED TECHNOLOGY BLADES	PERCENT IMPROVEMENTS
SEA LEVEL, STANDARD DAY			
THRUST AT TORQUE LIMIT, LB	18,856	19,867	5.4
ROTOR THRUST MARGIN, LB (2)	4,491	5,502	22.5
MAXIMUM OPERATNG WEIGHT, LB (1)	15,341	16,164	5.4
USEFUL LOAD, LB	6,181	7,004	13.3
MAXIMUM CRUISE SPEED, KNOTS (3)	308	322	5
4,000 FT, 95 F			
ROTOR THRUST MARGIN, LB	2,210	4,069	84.1
MAXIMUM OPERATING WEIGHT, LB (1)	13,485	14,998	11.2
USEFUL LOAD, LB	4,325	5,838	35.0

NOTE (1) ASSUMES 10.5% EQUIVALENT DOWNLOAD (INCLUDING ROTOR/ROTOR INTERFERENCE) AND 10% MANEUVER/MARGIN.
(2) AT DESIGN GROSS WEIGHT = 13,000 LB AND DESIGN MAX TORQUE = 163,000 IN. LB
(3) CALCULATED

TABLE 2. MATERIAL PROPERTIES AND APPLICATIONS

ELEMENT	MATERIAL	FIBER ORIENTATION	DENSITY (LB/IN3)	TENSION MODULUS (E) (PSIx10-6)	SHEAR MODULUS (G) (PSIx10-6)	ULTIMATE TENSILE STRENGTH (PSIx10-3)	FATIGUE ENDURANCE LIMIT AT R = 0.1 (PSI)
Spar Uni Nose Block Trailing Edge	Fiberglass	0°	0.067	6.3	0.5	200	14,000
Spar Uni	Graphite	0°	0.055	18.0	0.7	180	50,000
Outer Skin	Fiberglass	± 45°	0.067	2.0	1.67	20	2,680
Torsion Wrap	Graphite	± 45°	0.055	2.1	4.55	20	3,800
Core	Nomex	-----	2.0	-	-	-----	-----
Erosion Cap	Nickel	-----	0.322	25	9.5	114	28,500
Erosion Cover	Polyurethane	-----	0.045	0.3	-	-----	-----
Pitch Housing	Steel A151 4340	-----	0.283	29.0	11.0	150	25,000
Retention Pin	Steel PS-SPH CRES	-----	0.283	28.5	11.2	155	25,000
Lightning Protection Layer	Aluminized Fiberglass Cloth	0°,90°	0.06125	2.5	0.60	-----	-----
Lightning Protection Shield	Nickel 200	-----	0.321	23.7	12.0	-----	-----